ELSEVIER

Catalysis Today 64 (2001) 9–20

CATALYSIS TODAY

www.elsevier.com/locate/cattod

Catalytic partial oxidation of natural gas at elevated pressure and low residence time

L. Basini [a,*], K. Aasberg-Petersen [b,1], A. Guarinoni [a,2], M. Østberg [b,3]

[a] *Snamprogetti S.p.A., Via Maritano 26, 20097 San Donato Mil. (MI), Italy*
[b] *Haldor Topsøe A/S, Nymøllevej 55, DK-2800 Lyngby, Denmark*

Abstract

This work synthesizes the results of three kinds of experiment performed in order to investigate the molecular and temperature aspects of short residence time catalytic partial oxidation (CPO) of natural gas (NG), and the reaction at low- and high-pressure conditions.

Experiments performed in a reaction chamber equipped with IR and mass spectrometry have shown that CO and H_2 can be produced as primary reaction products with a selectivity close to 100%, by alternating flowing streams of CH_4 and O_2.

IR thermography and thermocouple measurements have measured large temperature gradients between the surfaces and the gaseous phase illustrating non-local thermal equilibrium conditions. These and other information have been useful for the design, construction and test of a bench-scale reactor where the possibility to perform the CPO reactions at pressures till 20 atm has been demonstrated.

Keywords: Catalytic partial oxidation of natural gas; DRIFT spectroscopy; IR thermography; Short contact time processes; High-pressure reactivity

1. Introduction

CPO has been the objective of many studies in the recent years. Before 1992, experiments had mainly been carried out at residence times around 1 s or above. At these conditions high temperatures, above 1300°C, were observed in the inlet zone caused by total combustion. The total combustion was followed by the methane steam reforming and shift reactions causing the temperature to decrease and the mixture to be in equilibrium at the exit of the catalytic bed [1,2].

In 1992, it was found [3,4] that CPO can occur at contact times of 10^{-3} s or less. In this case carbon monoxide and hydrogen can be produced directly, i.e. not via production of steam and carbon dioxide and temperature profiles of the catalytic beds do not show high temperature peaks [5–10]. However, most of the known studies on short residence time CPO have been carried out in laboratory scale reactors and only in one case it has been reported that the effect of pressure between 1 and 6 atm has been examined [9].

This work discusses the results of CPO experiments performed with Rh containing catalysts in three different experimental conditions. These have been designed in order to investigate: (a) molecular aspects of surface chemistry, (b) temperature aspects of the reaction environment and (c) the possibility to perform

* Corresponding author. Tel.: +39-2-520-56546; fax: +39-2-520-56757.
E-mail addresses: luca.basini@snamprogetti.eni.it (L. Basini), kap@topsoe.dk (K. Aasberg-Petersen), alessandra.guarinoni@snamprogetti.eni.it (A. Guarinoni), mro@topsoe.dk (M. Østberg).
[1] Tel.: +45-45-272401; fax: +45-45-272999.
[2] Tel.: +39-02-520-46780; fax: +39-02-520-56757.
[3] Tel.: +45-45-272756; fax: +45-45-272999.

0920-5861/01/$ – see front matter
PII: S0920-5861(00)00504-6

short residence time experiments under high-pressure high-temperature conditions.

The three experimental apparatus that have been used consisted of: (a) a reaction chamber equipped with DRIFT and mass spectrometry, (b) a laboratory scale plug flow reactor (PFR) equipped with IR thermography and thermocouples for solid and gas phases temperature mapping and (c) a bench-scale reactor where short contact time CPO has been experimented at a pressure of 20 atm.

The experiments performed in the reaction chamber equipped with IR and mass spectrometry have shown that CO and H_2 can be produced as primary reaction products with a selectivity close to 100%, by alternating reaction conditions with flowing streams of CH_4 and O_2. However, when CH_4 and O_2 have been contemporaneously admitted into the reaction environment, CO_2 and H_2O have also been formed through reactions involving surface species and gaseous O_2 molecules. Moreover, in agreement with previous studies [6,7,9] it has been found that CO_2 and H_2O formation has been reduced at high surface temperatures, suggesting that, at high temperatures, thermally activated desorption of primary reaction products (CO, H_2) has been prevailing versus total oxidation.

IR thermography and thermocouple measurements, performed in stationary conditions in a laboratory scale PFR, have shown that large temperature gradients between the surface and gaseous phase do exist. Moreover, comparisons between measured and calculated values have shown that surface temperatures exceed adiabatic temperatures while gas temperatures remain much lower. These findings are discussed by considering the occurrence of different reaction pathways along the catalytic bed and by considering phenomena that determine non-local thermal equilibrium between the solid and the gaseous phase.

Finally, bench-scale data have shown that hydrocarbon conversions in excess of 90% can be obtained at pressures up to 20 bars and at residence times around 10^{-2} s.

2. Experimental

2.1. Catalysts preparation

The preparation procedure and the characterization work of the used catalysts have been already given in [11,12]. Briefly it is reported here that the preparation method has involved a solid–liquid reaction between *n*-hexane solution of small Rh clusters and the powdered oxides (α-Al_2O_3, MgO and CeO_2). Rh content has been varied between 0.1 and 0.8 wt.% DRIFT spectra of the freshly prepared powdered materials showed carbonyl absorption bands (at ≈2090 and 2010 cm^{-1}) in all samples. These IR absorptions bands are assigned to $Rh^{I}(CO)_2$ species formed through an oxidative disaggregation of the tetra-metallic cluster.

2.2. Apparatus for spectroscopic and spectrometric studies

DRIFT and mass spectra in flowing gaseous environments have been collected at 0.1 MPa and temperatures between 25 and 750°C. The description of the equipment is reported in [11] and a scheme of the reaction chamber is reported in Fig. 1. DRIFT spectra have been recorded at a resolution of 4 $cm^{-1}$and signal to noise ratios have been reduced collecting between 300 and 500 scans with a procedure requiring between 2 and 3 min.

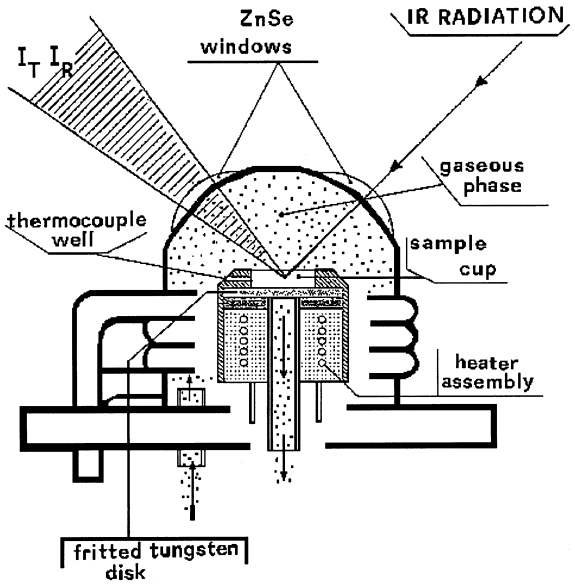

Fig. 1. Scheme of the reaction chamber equipped for DRIFT and mass spectrometry.

2.3. Apparatus for surface and gas temperature measurements

Temperature aspects of CPO reactions have been studied with a cylindrical tubular quartz PFR with an internal diameter of 15 mm and a wall thickness of 1 mm. The catalyst bed, filled with 1.5 g of regular α-Al_2O_3 spheres (Ø = 1 mm, Rh content = 0.32 wt.%) was 6 mm high. Gas temperatures have been monitored by two movable thermocouples located at the inlet and outlet of the catalytic bed. An IR camera (THERMOVISION 900 SW/TE) has been used for temperature measurements and analysis of both static and dynamic thermal patterns of the reacting catalyst. The camera has an internal compensation and self-calibration system based on two micro blackbodies and four temperature sensors. It is thermoelectrically cooled and it operates in the short-wave range 3–5 μm, suitable for high temperature applications. A filter "HT 1" (cut-on 3.82 μm, cut-off 3.9 μm) has widened the measurement range to 2000 K.

The system has been equipped with a 20° lens (Field of View, $H \times V = 20^\circ \times 12.5^\circ$; spatial resolution 2.5 mrad) and one close-up lens (spatial resolution 0.32 mrad corresponding to about 250 μm). The IR camera has been interfaced to a PC for the online acquisition of 12-bit digital images and data. Emissivity values have been adjusted with temperature-dependent equations derived from the literature.

The reactions have been ignited by a hot air beam impinging on the external wall of the catalytic bed. After ignition had taken place the reactions remained self-sustained. Reactants (H_2, He, O_2, CH_4) have been supplied from cylinders into different lines each equipped with a mass flow-meter and a controller. The composition of the output gas has been monitored with two HP gas chromatographs equipped with FID and TCD.

2.4. Bench-scale plant description

Main features of the experimental set-up are schematized in Fig. 2. The apparatus can be divided into four main sections: (1) a preheating/mixing section, (2) a reaction section (3) a gas cooling section and (4) a gas analysis section. NG and steam flows are mixed inside a pre-heater and subsequently with oxygen. CO_2 may be added to the NG as well as to the O_2 containing streams. The premixed feedstock enters a reactor made with steel walls (Incoloy 800H) with a thickness of 1 cm and with an internal refractory ceramic lining. Gaseous products have been bubbled inside a water filled tank cooled with a water jacket. Before entering the tank a small fraction of the product gases has been sampled. After condensation of water, the gas is sent to the sampling valve of the gas chromatographs (HP 5890) for the quantitative analysis of products. The exit streams from the quench barrel and from the GC analysis have been joined again and collected into a flow-meter and then into a vent line. The operating pressure has been kept constant by means of two control-valves placed downstream from the reactor.

The equipment, that contained between 10 and 30 ml of catalyst, has been used to perform reactivity tests at pressures between 1 and 20 atm and contact times between 5.0×10^{-3} and 3.5×10^{-2} s.

2.5. Thermodynamic calculation and estimates of adiabatic temperatures

The equilibrium temperatures of the water gas shift reaction (T_{WGS}) (1) the steam reforming reaction (T_{SR}) (2), and the CO_2 reforming reaction (T_{CR}) (3)

$$CO + H_2O = CO_2 + H_2 \quad (1)$$

$$H_2O + CH_4 = CO + 3H_2 \quad (2)$$

$$CO_2 + CH_4 = 2CO + 2H_2 \quad (3)$$

have been estimated according to the procedures of [16]. With Eqs. (4)–(6).

$$T_{WGS} = \frac{-\Delta G_{WGS}}{\ln(P_{CO_2} P_{H_2} / P_{CO} P_{H_2O})} \quad (4)$$

$$T_{SR} = \frac{-\Delta G_{SR}}{\ln(P_{CO} P_{H_2}^3 / P_{CH_4} P_{H_2O})} \quad (5)$$

$$T_{CR} = \frac{-\Delta G_{CR}}{\ln(P_{CO}^2 P_{H_2}^2 / P_{CH_4} P_{CO_2})} \quad (6)$$

Adiabatic exit temperatures for chemical systems at the thermodynamic equilibrium ($T_{ad.eq.}$) have been estimated using the Aspen Technology software Aspen Release 9.2.

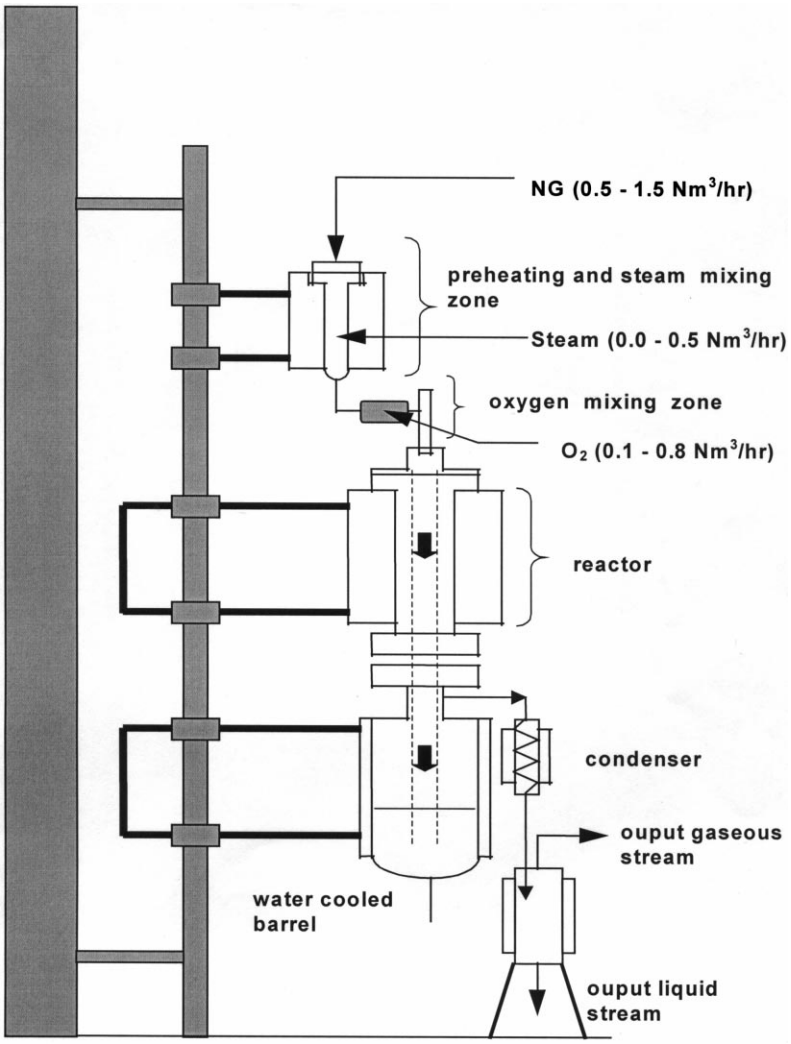

Fig. 2. Scheme of the bench-scale equipment constituted by a preheating-mixing, reaction and gas cooling sections.

Adiabatic exit temperatures corresponding to the experimental product compositions ($T_{ad.exp.}$) have also been calculated using procedures, enthalpy and heat capacity values given in [16].

3. Results

3.1. Molecular reactivity aspects

Fourteen experiments (schematized in Fig. 3) have been performed within an extensive research program, in order to investigate the molecular surface chemistry of Rh species with DRIFT and mass spectrometry. The detailed description of the experiments has already been given in [11–15]; here we will provide a synthesis of the results that have lead to a molecular description of some aspects of partial and total oxidation processes.

A number of reactions participate to CPO phenomena and the following ones have been investigated: (i) CO and CO_2 methanation (Experiments 1–8) [11,12], (ii) CO_2 reforming and water gas shift (Experiments 9 and 10) [13] and (iii) reactions between CH_4 and

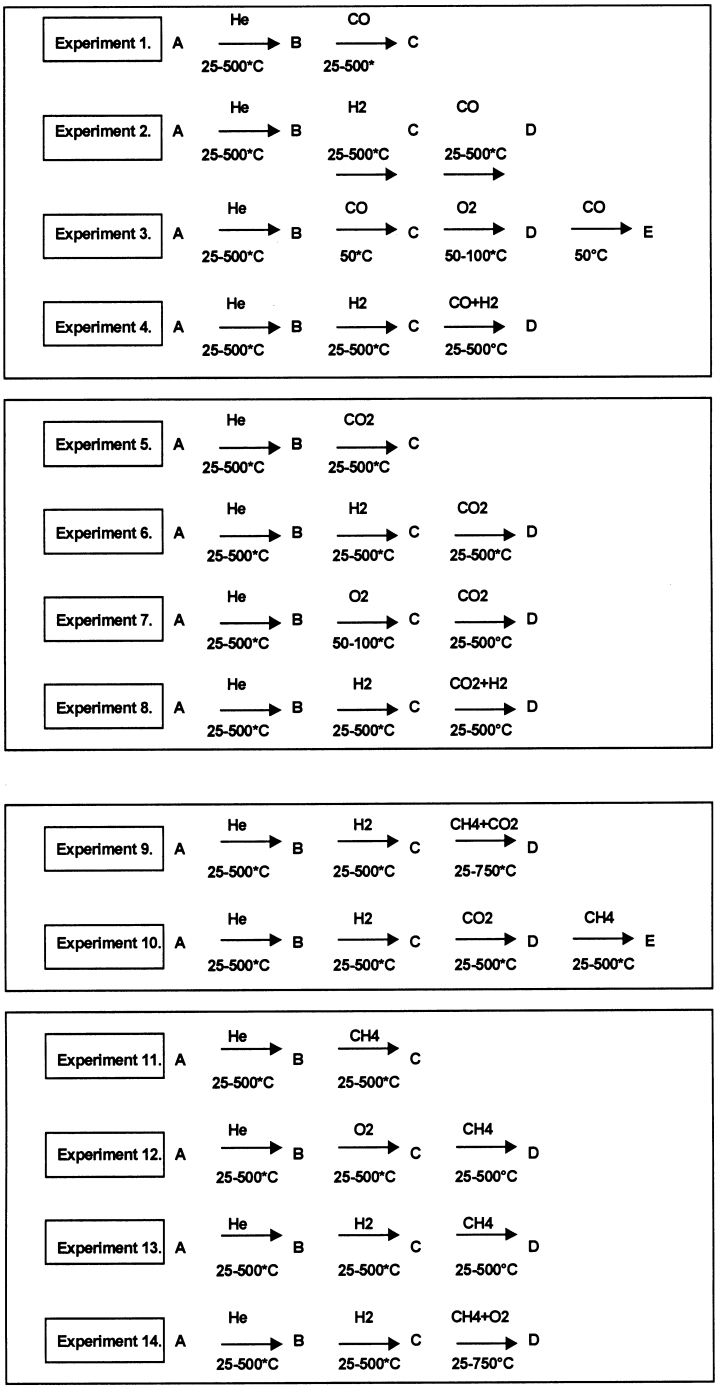

Fig. 3. Schemes of the experimental sequences performed to investigate aspects of surface Rh cluster chemistry.

gaseous or surface oxygen species (Experiments 11–14) [14,15].

In synthesis five Rh containing surface species have been identified; these are constituted by: (a) bare metallic clusters, (b) clusters containing highly reactive oxidic species, (c) clusters containing carbidic species, (d) carbonyl clusters and (e) hydridocarbonyl clusters.

The Rh clusters containing the highly reactive oxygen species could react with gaseous CH_4 producing hydridocarbonyl clusters. These could be subsequently thermally decomposed originating H_2 and CO with selectivity close to 100% [15]. H_2O and CO_2 could also be obtained as main reaction products by reacting the hydridocarbonyl clusters with oxygen.

Moreover, it has been found that a sequence of oxidative treatments and interactions with CH_4, performed at temperatures below 300°C, could generate a catalytic loop that consumed CH_4 and O_2 in separate steps producing only CO and H_2.

Fig. 4 schematically represents these reactivity features particularly showing that a common carbonyl complex can originate both total and partial oxidation products.

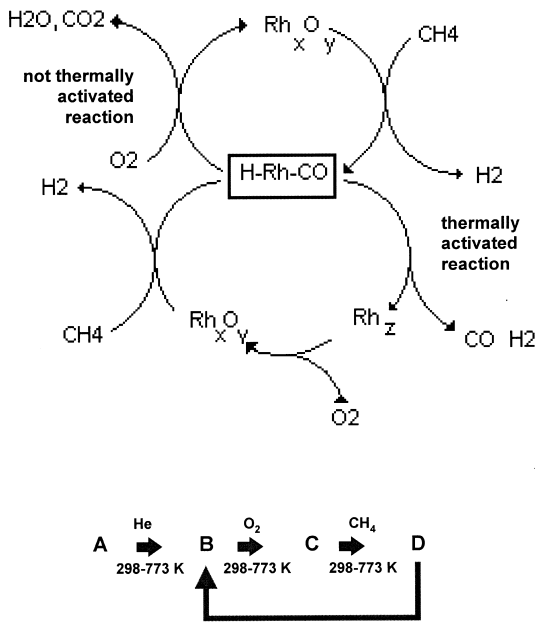

Fig. 4. Scheme of the reactivity characteristics detected with the DRIFT and mass spectrometry experiments indicating that a common hydridocarbonyl intermediate can originate partial and total oxidation products.

3.2. Thermochemical properties of the reaction environment

Reaction temperatures of the catalyst surfaces and of the gas phase have been investigated by performing the CPO reactions in a quartz PFR that contained 275 spherical pellets with a diameter of ca. 1 mm and with an overall Rh loading corresponding to 0.32 wt.%. The reactivity tests have been made with air as oxidant at $O_2/CH_4 = 0.50$–0.55 v/v.

Reaction ignition has been achieved by heating the external wall of the catalytic bed with a hot air beam. After ignition the hot air beam has been switched off and the reactions remained self-sustained.

The sequence of images of Fig. 5 shows how the ignition takes place using a premixed flow of air and CH_4 with $O_2/CH_4 = 0.1$ v/v. Only few spheres ignite initially and subsequently the reaction extends to the whole catalytic bed in about 1 min.

After this ignition step the O_2 flow has been gradually increased in order to achieve an O_2/C ratio of 0.50 v/v. Fig. 6 shows different IR thermography images taken at increasing O_2/CH_4 ratios.

Reactivity characteristics obtained under steady state conditions at two space velocity values are given in Table 1. Fig. 7 shows the surface temperature profile recorded for the two experimental conditions.

It is noted that surface temperatures have a steep increase at the beginning of the bed to values around 1100°C. The temperature increase is followed by a "plateau" whose extension is higher at the higher space velocity, then temperatures gradually decrease towards the end of the bed. In contrast, gas temperatures gradually increase from the entrance towards the end of the bed.

Table 1 also includes the measured surface and gas temperatures ($T_{surf.}$ and T_{gas}), the calculated equilibrium temperatures (T_{WGS}, T_{SR}, T_{CR}) and the calculated adiabatic temperatures ($T_{ad.exp.}$, $T_{ad.eq.}$) corresponding to the experimental and equilibrium product mixtures (see also Section 2). Interestingly, the comparison between calculated and experimental values shows that surface temperatures ($T_{surf.}$) have been higher than adiabatic temperatures that, in turn, have been higher than gas temperatures (T_{gas}).

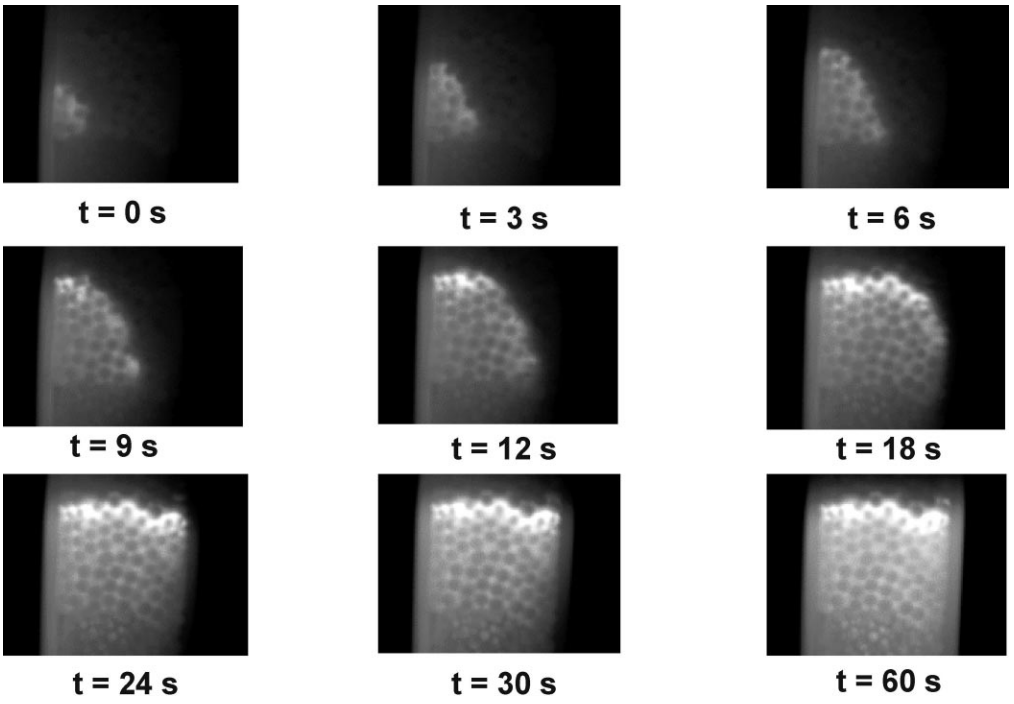

Fig. 5. Sequence of IR thermography images taken during the reaction ignition procedure at $O_2/CH_4 = 0.1$ v/v. The sequence shows that the reaction is ignited within a few particles and then is gradually propagated to the confining ones in about 60 s.

Moreover, it has been found that the equilibrium temperatures T_{WGS}, T_{SR}, T_{CR} are higher than T_{gas} but lower than $T_{surf.}$. It should also be noted that the adiabatic temperature is much higher than the exit gas temperature illustrating that a significant heat loss from the reactor has occurred. This is not surprising, since the reactor is a non-insulated quartz reactor with a very high external surface-to-volume ratio. In conclusion the experimental and calculated temperature values are ordered as follows:

$$T_{surf.} > T_{WGS} \cong T_{ad.\ exp.} > T_{SR},$$
$$T_{CR} \cong T_{ad.\ exp.} > T_{gas}$$

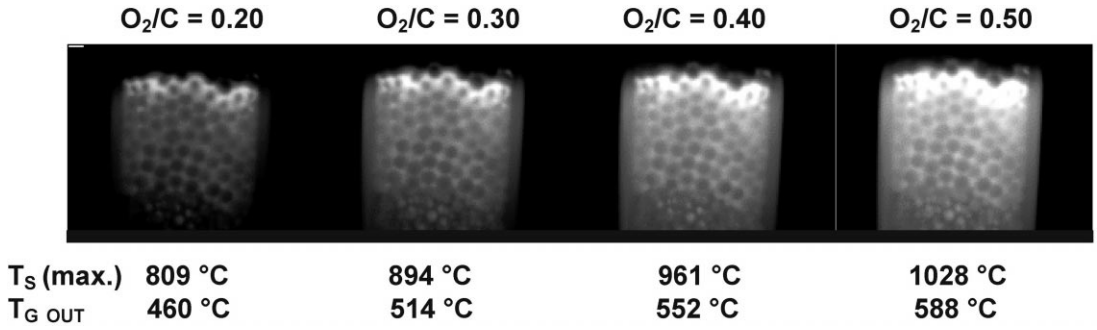

Fig. 6. Surface ($T_{surf.}$) and gas temperature (T_{gas}) values measured at increasing O_2/CH_4 during the start-up procedure (final GHSV = 199,444 Nl/kg/h).

Table 1
Operation parameters and reactivity features obtained under steady state conditions at two space velocity values in a quartz PFR equipped with IR thermography and thermocouples ($T_{surf.}$ surface temperature, T_{gas} gas temperature, T_{WGS}, T_{SR}, T_{CR}, water gas shift, steam reforming and CO_2 reforming equilibrium temperatures, $T_{ad.exp.}$ adiabatic temperature determined with inlet temperature and experimental inlet and outlet compositions, $T_{ad.eq.}$ adiabatic temperature calculated assuming equilibrium reactivity features)

O_2/C (v/v)	GHSV (Nl/kg/h)	CH_4 conv. (%)	O_2 conv. (%)	CO sel. (%)	H_2 sel. (%)	H_2/CO (v/v)	Run No.
0.5	200,556	80.1	99.9	91.5	87.3	1.91	1
0.5	500,000	85.0	99.6	94.2	88.5	1.88	2
T_{gas} (°C) in–out	$T_{surf.}$ max (°C)	T_{WGS} (°C)	T_{SR} (°C)	T_{CR} (°C)	$T_{ad.exp.}$ (°C)	$T_{ad.eq.}$ (°C)	Run No.
26–586	1012	858	705	723	942	753	1
27–699	1087	912	737	756	841	757	2

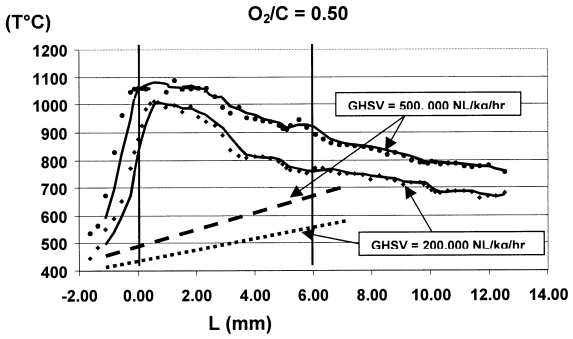

Fig. 7. Surface (continuous lines) and gas (dotted lines) temperature profiles measured under stationary reaction conditions at two space velocities. The two vertical lines delimit the positioning of the catalytic bed.

Turnover frequency (TF) values have also been estimated under these conditions and it has been found that TF_{CH_4} and TF_{O_2} have reached values, respectively, close to 200 and 100 s^{-1}.

These values have been calculated by determining the percentage (65%) of exposed Rh atoms on a sample discharged after 100 h of reaction with H_2 chemisorption. Moreover, it is noted that HRTEM analysis has not revealed the presence of Rh clusters on the fresh samples; but the same analysis performed on the spent catalyst, revealed the presence of a large number of Rh clusters whose diameters have been comprised between 10 and 60 Å.

3.3. HT–HP reactivity in the bench-scale plant

The high-pressure–high-temperature tests have been performed with oxygen and natural gas (NG) reactants. The NG source has had the composition given in Table 2. Start-up has been performed by pre-heating the NG and subsequently injecting the O_2 flow into the reaction environment with a O_2/C ratios determined in order to avoid the formation of a flammable mixture. Table 3 reports the reactivity

Table 2
Composition of natural gas used in the bench-scale experiments

Species	% v/v
CH_4	91.1
C_2H_6	2.8
C_3H_8	0.6
H_2	2.2
N_2	3.4

Table 3
A and B reactivity features obtained in the bench-scale reactor at 20 atm and GHSV = 200,000 Nl/kg/h at two different steam/carbon (S/C) values and comparison with the equilibrium reactivity characteristics calculated for an adiabatic reactor

	Experimental		Adiabatic equilibrium	
	A	B	C	D
P (atm)	20	20	20	20
T in (°C)	115	115	115	115
O_2/C (v/v)	0.58	0.5	0.58	0.58
S/C (v/v)	0.20	0.26	0.20	0.26
CO_2/C (v/v)	0.11	0.11	0.11	0.11
CH_4 conv. (%)	96.8	97.0	90.9	91.9
H_2 sel. (%)	83.3	84.8	90.8	88.8
CH_4 res. (%)	0.95	0.85	2.4	2.6
O_2 cons. (O_2 in/(H_2 + CO))	0.23	0.22	0.23	0.23
H_2/CO (v/v)	1.74	1.78	1.83	1.88
H_2/CO (v/v)	1.74	1.78	1.83	1.88
Tout ad. (°C)	941	989	948	966

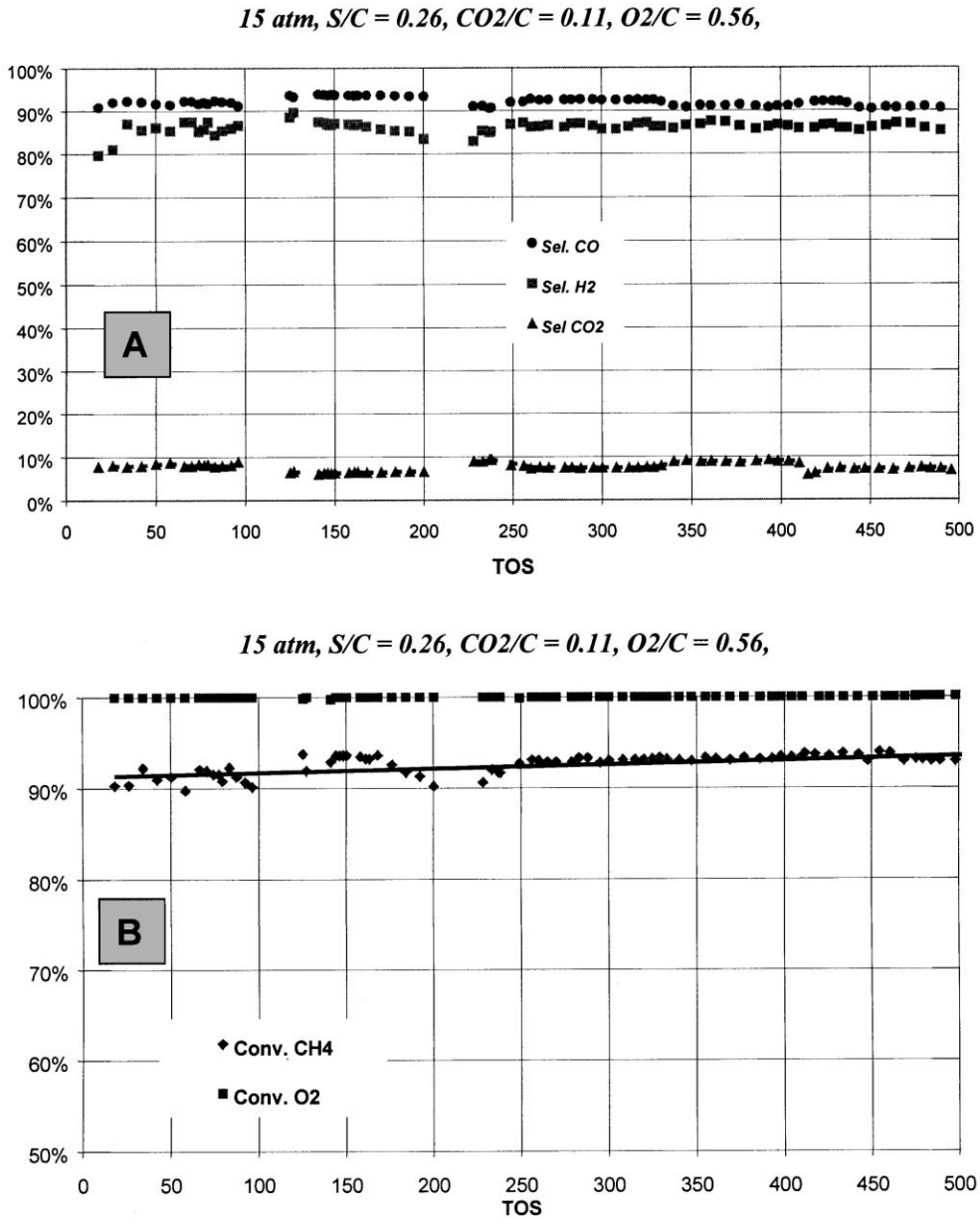

Fig. 8. Methane conversion (A) and selectivity towards synthesis gas (B) determined during a 500 h CPO reactivity test performed at 15 atm, GHSV = 120,000 h^{-1}, $O_2/C = 0.56$ v/v, $S/C = 0.3$ v/v, $CO_2/C = 0.13$ v/v.

characteristics of two experiments performed at 20 atm. Moreover, Table 3 compares the experimental results with the ones estimated for an equilibrium adiabatic reactor.

One 500 h reactivity test has also been performed at 15 atm, GHSV = 180,000 Nl/kg/h, $O_2/C = 0.56$ v/v, $S/C = 0.30$ v/v, $CO_2/C = 0.26$ v/v. Fig. 8A and B shows that constant selectivity towards H_2

and CO and methane conversion values have been obtained.

4. Discussion

The formation of surface hydridocarbonyl complexes and of gaseous CO and H_2 and not of CO_2 and H_2O, when gaseous CH_4 has been made interact with surface sites previously exposed to oxygen molecules sustains the possibility to obtain partial oxidation of methane with a direct mechanism.

The formation of CO_2 and H_2O is observed only when the surface hydridocarbonyl clusters are exposed to gaseous oxygen. This suggests that total and partial oxidation products can be obtained by the same surface intermediate.

The prevailing of partial versus total oxidation products, under stationary reaction conditions and using premixed reactant flows, should depend on the results of the competition between thermal decomposition of the hydridocarbonyl clusters and their reaction with gaseous oxygen.

It is worth briefly to mention that the direct formation of CO and H_2 is also observed with molecular dynamics studies performed under nearly collision free conditions. These studies were aimed at generating primary product molecules (at an equivalent pressure of $\cong$0.1 Pa) desorbing from the surfaces without suffering of collisions with incoming reactants.

Kunimori et al. [17–19] studied, with this experimental approach, the oxidation of C_2–C_4 hydrocarbons. They found that CO and H_2 are formed as primary products with an extremely high selectivity at surface temperatures higher than 750°C, when thermally activated desorption of primary reaction products is favored versus not thermally activated total oxidation. We obtained analogous results by studying the partial oxidation of CH_4 [4] even at extremely high O_2/CH_4 molar ratios ($O_2/CH_4 = 0.5$–5 v/v). These indications are in agreement with the observation of other authors reported in [9].

It worth also to mention that several kinetic analysis performed with temporal analysis of the reaction products (TAP) have investigated if CO and H_2 can be directly produced from CH_4 and O_2.

However, these analysis have not always reached the same conclusions.

For instance Mollens et al. [20,21] have performed a very detailed experimental study on the reactivity features produced on Pt and Rh sponges, concluding that CO and H_2 can be desorbed as primary products with a Mars–van Krevelen mechanism including the reduction of noble metal oxide surface species with gaseous CH_4 and reoxidation with O_2.

Instead Buyevskaya et al. [22] studying the same reactions on 1 wt.% Rh/γ-Al_2O_3 concluded that CO is a secondary reaction product formed by surface reaction between carbon deposits and CO_2, which are the primary reaction products. In situ DRIFT studies performed by the same authors [23] also concluded that surface OH groups are involved in the CH_4 conversion to CO via reforming reactions.

Despite these discrepancies on the results of the TAP experiments there are a number of results indicating that high surface temperature values are crucial for the fast achievement of partial oxidation products with a direct mechanism. Among these we mention the experimental observation made with optical pyrometers revealing the occurrence of hot spot phenomena that generated reaction environments with high local temperatures [24–27] and non-equilibrium reactivity features.

Accordingly, the experiments performed in the PFR reactor equipped with IR thermography have detected surface temperatures higher than the gas temperatures and than the adiabatic equilibrium temperatures all along the catalytic bed.

This condition could be due to the fact that mass transfer proceeds more rapidly than heat transfer. However, in our experiments, Lewis number values (ratio between heat transfer to mass transfer) have been above 1. This should exclude that heat transfer limitation could explain the temperature rise.

Instead, we believe that: (i) the temperature difference between the gas and the solid phase, (ii) the occurrence of surface temperatures higher than the adiabatic ones all along the catalytic bed and (iii) the characteristics of the observed axial temperature profiles could be explained with two kinds of phenomena that we introduce in a qualitative manner.

[4] Experiments were performed with G.L. Haller and C. Wey at the Department of Physical Chemistry of Yale University.

These phenomena have a chemical and a physical nature and particularly they are related to the occurrence of: (i) a non-homogeneous chemical reactivity along the catalytic bed and (ii) an uneven distribution of the radiative reaction heat between the solid and the gaseous phase.

The characteristics of the non-homogeneous reaction environment can be discussed considering the system composed by the chemical equations including the WGS (1) the steam and CO_2 reforming (2) and (3) and the total (7) and partial oxidation (8)

$$CH_4 + 2O_2 \rightarrow CO_2 + 2H_2O,$$
$$\Delta H^0 = -191.8\,\text{kcal/mole} \quad (7)$$

$$CH_4 + \tfrac{1}{2}O_2 \rightarrow CO + 2H_2,$$
$$\Delta H^0 = -8.5\,\text{kcal/mole} \quad (8)$$

This system comprises strongly exothermic and endothermic reactions that can be localized in different zones of the catalytic bed. Total combustion (7) is the most competitive reaction at the very beginning of the catalytic bed in conditions of "low temperature" and high oxygen partial pressure. Total combustion determines a strong energy release and a fast temperature rise. WGS, steam and CO_2 reforming (1)–(3) are secondary reactions and are preferentially localized in the tail section of the bed determining a temperature reduction.

However, it is noted that the initial contribution of total oxidation could be reduced at very short contact time conditions under a mass transfer limited regime. This would allow to a portion of the incoming reactants to pass unconverted throughout the total combustion zone reaching a high temperature environment with a relatively low partial pressure of oxygen where direct partial oxidation would be favored.

The temperature difference between the solid and the gaseous phase could be instead explained by considering that: (i) chemical reactions remain largely confined to the gas–solid inter-phase zone, while the gas phase remains chemically cool, (ii) the solid absorbs the reaction heat much better than the gas phase.

The heat absorption characteristics of the solid could also determine the achievement of excess enthalpy conditions and of surface temperature values higher than the adiabatic values. The gas should instead be gradually heated along the bed due to desorption of hot reaction products and due to the collisions with the hot surfaces.

The occurrence of excess enthalpy conditions at the solid–gas inter-phases have been initially proposed by Weinberg et al. [28–31] in the late sixties. Lately, these phenomena were experimentally verified in flameless ceramic combustors and described with physical and mathematical models. The experimental and modeling issues are reviewed in [32,33].

In conclusion it is noted that Table 1 shows that the equilibrium temperature of the water gas shift (T_{WGS}) reaction has a higher value than the steam reforming (T_{SR}) and the CO_2 reforming (T_{CR}) equilibrium temperatures. This indicates that the short residence time CPO process has occurred under kinetically controlled conditions where steam and CO_2 reforming have played a minor role in comparison to water gas shift.

The results of the bench-scale experiments indicate that these reactivity features can also be maintained for a reasonable time without catalyst deactivation in high-pressure conditions.

In particular, it is noted that in the cases reported in Table 3, the experimental conversion of methane is above the equilibrium conversion estimated for an adiabatic reactor. Furthermore, the selectivity of CO is close to the one predicted for equilibrium conditions while the H_2 selectivity remains lower. However, it cannot be excluded that this surprising observation is caused by experimental uncertainties and further work is in progress to ascertain the veridicality of the result.

5. Conclusions

Experiments performed in a reaction chamber equipped with IR and mass spectrometry have shown that CO and H_2 are produced as primary reaction products through thermal decomposition of surface carbonyl species with a selectivity close to 100%. The same surface species could also originate H_2O and CO_2 by interacting with gaseous oxygen molecules. CO_2 and H_2O formation has been reduced at high surface temperatures, suggesting that at high temperatures thermally activated desorption of primary

reaction products (CO, H_2) has been prevailing versus total oxidation.

IR thermography and thermocouple measurements have shown large temperature gradients between surfaces and gaseous phases. Comparisons between experimental temperatures and calculated adiabatic temperatures have shown that short residence time CPO is occurring in an excess enthalpy inter-phase environment. The occurrence of this environment is probably responsible for the high reaction rates.

Bench-scale experiments have demonstrated the possibility to perform the SCT–CPO of NG at pressures till 20 atm and to sustain the reactions without deactivation for 500 h at 15 atm.

References

[1] M. Prettre, Ch. Eichner, M. Perrin, Trans. Faraday Soc. 43 (1946) 33.
[2] D. Dissanayake, M.P. Rosinek, K.C.C. Kharas, J.H. Lunsford, J. Catal. 132 (1991) 117–127.
[3] H. Hickman, L.D. Schmidt, J. Catal. 138 (1992) 267–282.
[4] V.R. Choudary, A.S. Mamman, S.D. Sansare, Angew. Chem. Int. Ed. Engl. 31 (1992) 1189–1190.
[5] A.S. Bodke, S.S. Bharadwaj, L.D. Schmidt, J. Catal. 179 (1998) 138.
[6] D.A. Hickman, L.D. Schmidt, Science 259 (1993) 343–346.
[7] L.D. Schmidt, O. Deutschmann, C.T. Goralski Jr., Stud. Surf. Sci. Catal. 119 (1998) 685.
[8] L. Basini, A. Guarinoni, K. Aasberg-Petersen, Stud. Surf. Sci. Catal. 119 (1998) 699.
[9] A.G. Dietz, L.D. Schmidt, Catal. lett. 33 (1995) 15.
[10] F. Basile, L. Basini, M. D'Amore, G. Fornasari, A. Guarinoni, D. Matteuzzi, G. Del Piero, F. Trifirò, A. Vaccari, J. Catal. 173 (1998) 247–256.
[11] L. Basini, M. Marchionna, A. Aragno, J. Phys. Chem. 23 (1992) 9431.
[12] L. Basini, A. Aragno, J. Chem. Soc., Faraday Trans. 90 (1994) 787.
[13] L. Basini, D. Sanfilippo, J. Catal. 157 (1995) 162.
[14] L. Basini, A. Aragno, G. Vlaic, Catal. Lett. 39 (1996) 49.
[15] L. Basini, A. Guarnoni, A. Aragno, J. Catal. 190 (2000) 284.
[16] J. Kjaer, in: Computer Methods in Gas Phase Thermodynamics, Haldor Topsoe, Vedbaek, 1972.
[17] K. Watanabe, H. Uetsuka, H. Ohnuma, K. Kunimori, Stud. Surf. Sci. Catal. 101 (1996) 891.
[18] H. Uetsuka, K. Watanabe, T. Iwade, K. Kunimori, J. Chem. Soc., Faraday Trans. 91 (1995) 1801.
[19] K. Kunimori, H. Uetsuka, T. Iwade, T Watanabe, S. Ito, Surf. Sci. 283 (1993) 58.
[20] E.P.J. Mallens, J.H.B.J. Hoebink, G.B. Marin, Catal. Lett. 33 (1995) 291.
[21] E.P.J. Mallens, J.H.B.J. Hoebink, G.B. Marin, J. Catal. 167 (1997) 43.
[22] O.V. Buyevskaya, D. Wolf, M. Baerns, Catal. Lett. 29 (1994) 249.
[23] K. Walter, O.V. Buyevskaya, D. Wolf, M. Baerns, Catal. Lett. 29 (1994) 261.
[24] D. Dissanake, M.P. Rosinek, J.H. Lunsford, J. Phys. Chem. 97 (1993) 3644.
[25] Y.F. Chang, H. Heinemann, Catal. Lett. 21 (1993) 215.
[26] Y. Matsumura, J.B. Moffat, Catal. Lett. 24 (1994) 59.
[27] F. Basile, L. Basini, M. D'Amore, G. Fornasari, A. Guarinoni, D. Matteuzzi, G. Del Piero, F. Trifirò, A. Vaccari, J. Catal. 173 (1998) 247.
[28] F.J. Weinberg, Advanced Combustion Methods, Academic Press, New York, 1988, p. 183.
[29] S.A. Loyd, F.J. Weinberg, Nature 251 (1974) 48.
[30] J.S. Fox, Combust. Sci. Technol. 12 (1976) 147.
[31] F.J. Weinberger, Nature 233 (1971) 239.
[32] J.R. Howell, M.J. Hall, J.L. Ellzey, Prog. Energy Combust. Sci. 22 (1996) 121.
[33] J.G. Hoffamnn, R. Echigo, H. Yoshida, S. Tada, Combust. Flame 111 (1997) 32.